August 27-31, 2023
FLORENCE - ITALY
ICWE 16
16th International Conference on Wind Engineering

Effect of the accelerating flow on a square cylinder

A. Mariotti[1], G. Lunghi[1], S. Brusco[2,3], G. Piccardo[3], M.V. Salvetti[1]

[1]*Dipartimento di Ingegneria Civile e Industriale, University of Pisa, Italy,*
alessandro.mariotti@unipi.it, gianmarco.lunghi@phd.unipi.it, maria.vittoria.salvetti@unipi.it
[2]*Faculty of Engineering, Western University, London, Canada sbrusco@uwo.ca*
[3]*Dipartimento di Ingegneria Civile, Chimica e Ambientale, Polythecnic School, University of Genoa, Italy, giuseppe.piccardo@unige.it*

SUMMARY:
The present work investigates the high-Reynolds accelerating flow around a square cross-sectional cylinder, a classic shape of interest for wind-engineering applications, e.g. towers and skyscrapers. The flow is characterized by the shear-layer separation at the upstream edges. The separated shear layers undergo to Kelvin-Helmholtz instability, but they do not lose coherence until they form the von Karman vortex street in the wake. Regarding the mean flow features, no reattachment is found on the cylinder lateral surface. We perform high-fidelity Large-Eddy Simulations (LES) to investigate the effect of Gaussian-type inflow accelerations of different intensities from $Re = 1.72 \times 10^4$ to $Re = 6.536 \times 10^4$. LES results are compared and validated against the experiments in Brusco et al. (2022) and an excellent agreement is found between the results of experiments and LES. Numerical simulations allowed us to have further insights into the vortex-shedding phenomenon and the behavior of the force acting on the square cylinder during the flow acceleration. Moreover, a parametric study is performed by considering different inflow-acceleration intensities to reproduce conditions similar to full-scale thunderstorm outflows. Constant-frequency time cells are found in the vortex-shedding from a square cylinder for all the investigated acceleration levels. The behavior of the time cells is characterized using time-frequency analysis based on the wavelet transform.

Keywords: Square cylinder, Gaussian-type acceleration, Large-Eddy Simulations

1. INTRODUCTION

The square cross-section is a classic shape for wind-engineering applications, e.g. high-rise buildings and towers, and the flow characteristics for constant inflow conditions have been widely investigated. The flow is characterized by upstream-edge separation. The separated shear layers undergo Kelvin-Helmholtz instability, but they do not lose "coherence" until they roll up in the classical von Karman vortex shedding in the wake. The mean flow does not reattach on the cylinder side. Square cylinders with constant-velocity inflow conditions have been widely investigated in the literature, and no significant changes in flow topology and dynamics are found within the range $Re \simeq 10^3 - 10^6$ (see, e.g., Bruno and Oberto, 2022; Rodi, 1997; Trias et al., 2015). On the other hand, most of the literature proposes even sophisticated analyzes of the structural response to non-stationary flows but considers the aerodynamics of the body as in stationary flows, having no reference database for accelerating/decelerating flows. Only in some cases, the effect of wind acceleration has been experimentally and numerically investigated considering inlet acceleration starting at rest (Guo et al., 2021; Yang and Mason, 2019) and showing that the shear-layer

dynamics and the vortex-shedding frequency are sensitive to the variation of the inflow velocity. More recently, typical conditions of realistic scenarios presenting flow accelerations and decelerations starting from a non-zero velocity were studied, in the framework of the ERC THUNDERR project, in the wind-tunnel tests by Brusco et al. (2022). In particular, Brusco et al. (2022) studied the effects of Gaussian-type inflow accelerations and decelerations on a square cylinder in the Reynolds range $Re = 1.72 \times 10^4 - 6.34 \times 10^4$, observing constant-frequency time cells in the vortex-shedding.

In the present work, the effects of different inflow accelerations on the flow dynamics around a square cylinder and on the related vortex-shedding frequencies have been numerically studied. First, a Large-Eddy Simulation has been carried out for the same flow acceleration as in the experiments in Brusco et al. (2022) for cross-validation. Then, we perform a parametric study for different acceleration intensities to consider also more severe events. These simulations may be considered a first step toward the characterization of the wind loads on civil buildings due to thunderstorm outflows and to a better appraisal of the limits of the wind-load predictions obtained under the assumption of steady-wind conditions.

2. PROBLEM DEFINITION AND NUMERICAL METHODOLOGY

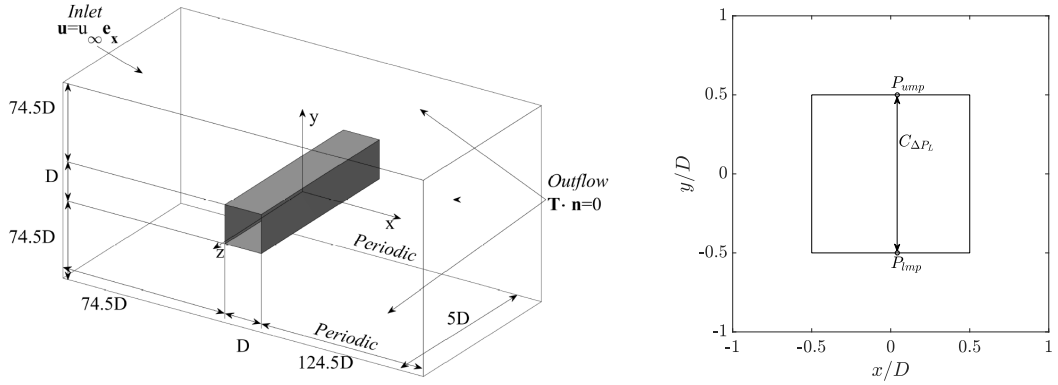

Figure 1. Sketch of the computational domain and boundary conditions (left) and of the cross-section $z/D = 0$ and pressure tap distribution (right).

We consider the incompressible flow around a square cylinder at zero angles of attack. Large-Eddy Simulations are performed by using the open-source code Nek5000, based on a high-order spectral element method. Each spectral element is rectangular and the basis functions inside the elements are Legendre polynomials of order N for velocity and $N-2$ for pressure in each direction; $N = 6$ has been used in this work, as in Lunghi et al. (2022) and Mariotti et al. (2017). A third-order backward finite-difference scheme based on the high-order splitting method is used for time advancing. The computational domain is sketched in Fig. 1a, together with the cylinder cross-section and the reference system in Fig. 1b. The cylinder center is located at $x/D = y/D = 0$, being D the width of the square cylinder, and the computational domain spans the following dimensions: $-75 \leq x/D \leq 125$, $-75 \leq y/D \leq 75$ and $0 \leq z/D \leq 5$. The spectral element size and distribution are the same used in Lunghi et al. (2022) and Mariotti et al. (2017). In particular, the element size in the streamwise and lateral directions is $\Delta x/D = \Delta y/D = 0.125$ near the cylinder, while the element size is uniform in the spanwise direction, $\Delta z/D = 0.558$. A quadratic filter is applied to the three

highest spectral modes. The effect of the filter can be considered as a subgrid-scale dissipation (see, e.g., Mariotti et al., 2017). A uniform unsteady velocity profile with no turbulence (smooth flow) is imposed at the inlet. The time histories of the inflow Reynolds number, Re, and of the acceleration made non-dimensional by using the inlet velocity at time $t = 0$, $aD/u^2_{\infty,0}$, are reported in Fig. 2a and Fig. 2b, respectively. Dotted vertical lines delimit the acceleration regions. First, the same unsteady flow condition as in the experiments in Brusco et al. (2022) is considered for cross-comparison. The inflow Reynolds number varies from $Re = 1.720 \times 10^4$ to $Re = 6.536 \times 10^4$ with a Gaussian-type acceleration. In the reference experiment, the maximum non-dimensional acceleration is equal to 2.35×10^{-2}. Moreover, two additional LES are carried out for inflow Reynolds number varying in the same range as the experiments with higher accelerations equal to $1.33 \times a_{ref}$ and $2 \times a_{ref}$. In all the LES, the no-slip condition is imposed at the body surface and traction-free boundary conditions for both the outflow and the upper and lower boundaries of the domain, and periodicity is imposed in the spanwise direction.

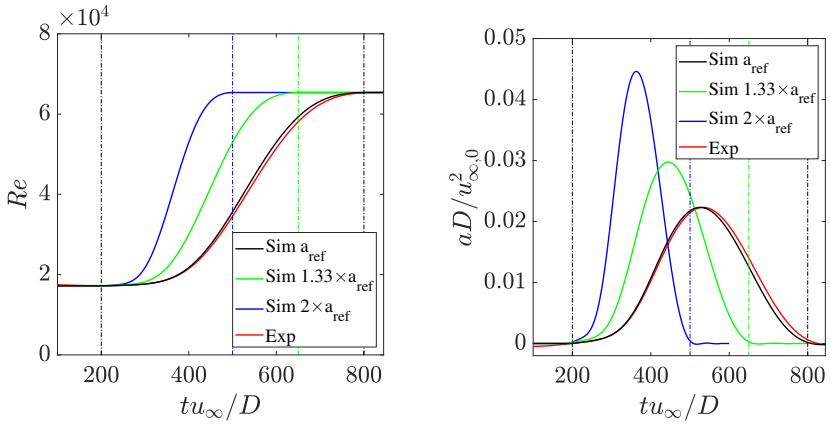

Figure 2. Time behavior of the inflow Reynolds number (left) and acceleration (right). Experiment from Brusco et al. (2022).

3. RESULTS AND DISCUSSION

In Figure 3a we compare the experimental and numerical time histories of the differential-pressure coefficients in crossflow directions. This coefficient is defined as in Fig. 1b and, as explained in Brusco et al. (2022), it is directly related to the lift coefficient. The numerical simulation provides a result in overall good agreement with the experiment by Brusco et al. (2022). In particular, the numerical coefficient presents almost identical oscillations with the experiment. The oscillation cycles have periods decreasing in time with the increasing inflow velocity. It follows that the vortex-shedding frequency increases with the increase of inlet velocity. Its behavior is characterized by using a time-frequency analysis based on the continuous wavelet transform. For our purpose, we use a complex Morlet wavelet with a central frequency of 6π and we derived from the wavelet energy maps the ridges indicating the vortex-shedding frequency, n^*, at each time window. The same discrete changes in the vortex-shedding frequency as in the experiments in Brusco et al. (2022) are found in the numerical simulations, with the presence of constant-frequency time cells (see Fig. 3b). The corresponding Strouhal number witnesses a decrease within the time cells, followed by a sudden increase between the cells, pointing out the presence of discontinuities in an even more glaring way (see Fig. 4a). The vortex-shedding Strouhal number is always inside the

range $0.10 \leq St \leq 0.14$, and the agreement between LES and experiment is again satisfactory. The increasing intensity of the acceleration reduces the time length of the time cells, and it decreases the vortex-shedding Strouhal number inside each cell, but a similar behavior of the Strouhal is found if considering the Reynolds number (see Fig. 4b). Further details on pressure distributions, force coefficients, and the variation of the vortex-shedding Strouhal number with time and with the Reynolds number will be given in the final presentation.

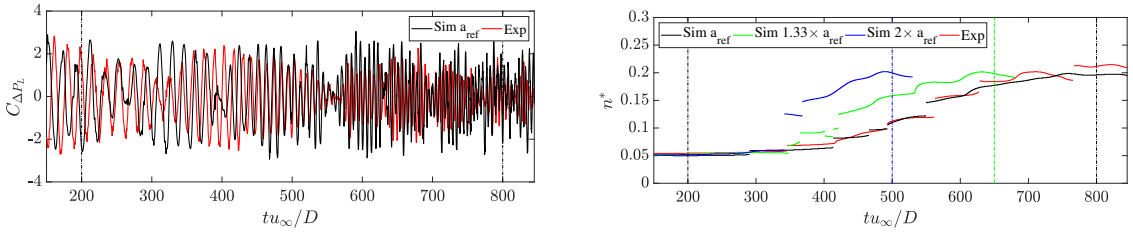

Figure 3. Time behavior of the crossflow differential-pressure coefficients (left) and of the vortex-shedding frequency (right). Experiment from Brusco et al. (2022).

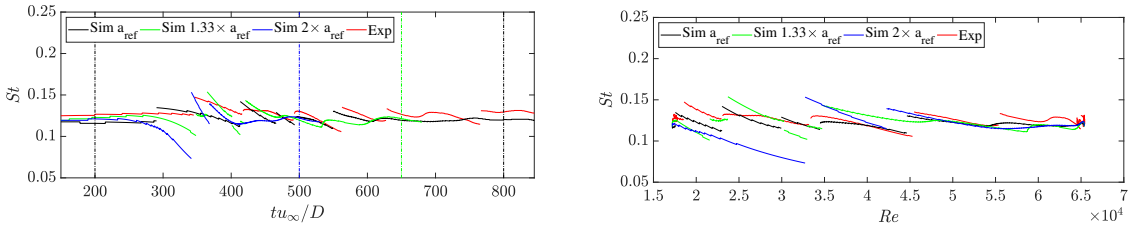

Figure 4. Vortex-shedding Strouhal number as a function of time (left) and Reynolds (right). Experiment from Brusco et al. (2022).

REFERENCES

Bruno, L. and Oberto, D., 2022. Effects of cell quality in grid boudary layer on the simulated flow around a square cylinder. Comput. Fluids 238, 105351.

Brusco, S., Buresti, G., Lo, Y. L., and Piccardo, G., 2022. Constant-frequency time cells in the vortex-shedding from a square cylinder in accelerating flows. J. Wind Eng. Ind. Aerod. 230, 105182.

Guo, F., Wu, G., and Du, X., 2021. Numerical investigation of flow around a square cylinder in accelerated flow. Phys. Fluids 33, 104105.

Lunghi, G., Pasqualetto, E., Rocchio, B., Mariotti, A., and Salvetti, M. V., 2022. Impact of the lateral mean recirculation characteristics on the near-wake and bulk quantities of the BARC configuration. Wind Struct. 34(1), 115–125.

Mariotti, A., Siconolfi, L., and Salvetti, M. V., 2017. Stochastic sensitivity analysis of large-eddy simulation predictions of the flow around a 5:1 rectangular cylinder. Eur. J. Mech. B/Fluids 62, 149–165.

Rodi, W., 1997. Comparison of LES and RANS calculations of the flow around bluff bodies. J. Wind Eng. Ind. Aerod. 69-71, 55–75.

Trias, F. X., Gorobets, A., and Oliva, A., 2015. Turbulent flow around a square cylinder at Reynolds number 22,000: A DNS study. Comput. Fluids 123, 87–98.

Yang, T. and Mason, M., 2019. Aerodynamic characteristics of rectangular cylinders in steady and accelerating wind flow. J. Fluids Struct. 90, 246–262.